

Theory and Simulation of DNA Charge Transfer: From Junctions to Networks

Tobias Cramer,[†] Antonio Volta,[‡] Alexander Blumen,[‡] and Thorsten Koslowski^{*,†}

Theoretische Polymerphysik and Institut für Physikalische Chemie, Universität Freiburg, Albertstrasse 23a, D-79104 Freiburg im Breisgau, Germany

Received: June 25, 2004; In Final Form: August 18, 2004

In this work, we address charge transfer within complex arrangements of nucleobases from a theoretical and numerical point of view. We study dendrimers constructed from T-shaped double-stranded DNA three-way junctions (3WJs). The electronic structure of these junctions is computed on an atomistic level using a chemically specific Su–Schrieffer–Heeger Hamiltonian, which has been extended by a nonretarded reaction field to take solvent polarization effects into account. Hopping rates through isolated 3WJs are derived by analyzing the emerging potential energy surfaces using Marcus' theory of charge transfer. We find highly anisotropic transport; the corresponding rates are used to compute the global trapping kinetics on DNA dendrimers with a central absorbing core. As a potential application, we discuss a DNA-based drug delivery system.

1. Introduction

Recent years have seen two important developments in the physics and chemistry of deoxyribonucleic acid (DNA). First, charge transport within the biopolymer has become an important issue. Experimental and theoretical studies have been motivated by the attempt to understand the mechanisms of DNA damage and repair and by potential applications in sensors or nano-devices.^{1–4} In a series of landmark photochemical studies, Barton and co-workers have pioneered charge mobility studies in DNA by intercalating donor and acceptor complexes into DNA strands.⁵ The analysis of the photochemical kinetics—now possible down to the femtosecond range⁶—has helped to gain a deeper understanding on the mechanism of charge transfer in the excited state. More recently, Giese and co-workers have oxidatively created holes in DNA and have studied their migration by analyzing the products resulting from the consecutive cleavage reactions.⁷ In a different type of experiment, a DNA strand is connected to two electrodes;⁸ whether DNA may operate as a nanowire enabling coherent charge transfer in this setup is still a matter of dispute.⁹

Second, the study of DNA topologies beyond a linear sequential arrangement of nucleobases has been enabled by considerable progress both in synthetic methods and in structural analysis. Three-way junctions (3WJs) and four-way junctions (4WJs) feature as central elements in the synthesis of complex DNA molecules. These objects include DNA cubes,¹⁰ octahedra,¹¹ networks,¹² or dendrimer-like arrangements.^{13,14} As the simplest structure that supports nonlinear DNA topologies, a 3WJ is displayed schematically in Figure 1. It consists of three single-stranded DNA chains (AB5', CA'5', and B'C'5', where each of the capital letters represents an individual sequence of nucleobases). With A, B, and C being complementary to A', B', and C', respectively, the three strands organize themselves into a 3WJ. Protruding 5'—or, alternatively, 3'—sequences can

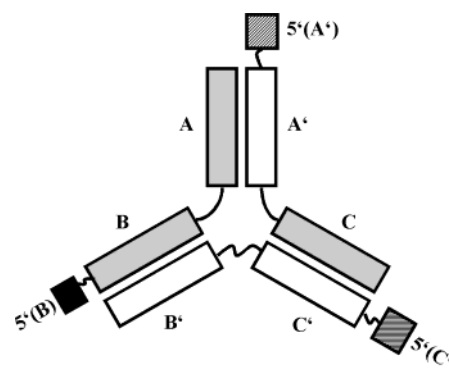


Figure 1. Arrangement of the DNA building blocks A, B, and C, and their complements A', B', and C', in a three-way junction (3WJ). AB5'-(B), B'C'5'-(C'), and 5'(A')A'C are assumed to be synthesized as single-stranded DNA, where the protruding 5' ends serve as links to other three-way junctions. For further details, see text and ref. 13.

be designed to enforce the arrangement of the DNA oligomers into specific topologies. As an impressive example, we consider the rational synthesis of a DNA dendrimer with a diameter of ~70 nm by Luo and co-workers.¹³ 3WJs may not only feature as a structural motive in DNA polymer design, but also may have an important biochemical role in the structure of tRNAs or in the genome of certain viruses.¹⁵

In this work, we consider the phenomenon of DNA charge transfer in connection with the possibility to design complex DNA topologies. In particular, we theoretically analyze charge migration processes through DNA dendrimers. Our study has been partly motivated by recent experiments on related systems,^{16,17} and the work is organized as follows: In the next section, we focus on a 3WJ structure that has been determined by NMR spectroscopy^{18,19} and the description of DNA charge transfer in the framework of an atomistic, chemically specific theory.^{20,21} The rates thus obtained for hole transfer through a 3WJ will be used in the third section to analyze the global kinetics of charge transfer and its side reaction, DNA cleavage, in nanosized dendrimeric arrangements of 3WJs. We discuss potential applications to drug- or DNA-delivery systems. Conclusions will be derived in the final section.

* Author to whom correspondence should be addressed. Fax: (+49)-761-203-6189. E-mail address: Thorsten.Koslowski@physchem.uni-freiburg.de.

[†] Institut für Physikalische Chemie.

[‡] Theoretische Polymerphysik.

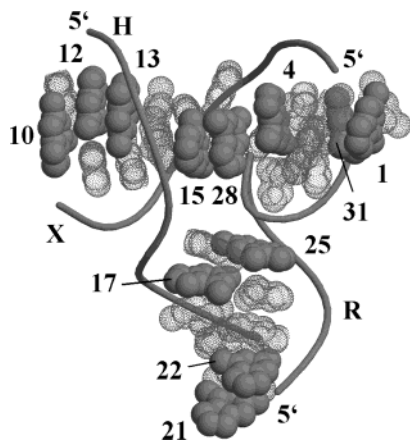


Figure 2. Model of the three-way junction 1EKW, after the NMR structure of refs 18 and 19. Guanines are drawn as solid spheres and are labeled; other nucleobases are shown as dotted spheres. The three backbone strands are represented by three solid lines, which have been labeled and whose orientation is shown.

2. Charge Transfer within a Three-Way Junction

Although many examples of 3WJs have been synthesized,¹⁵ structural information on these entities is sparse and, to our knowledge, restricted to two NMR studies of small oligomers.^{18,19,22,23} For reasons that will become apparent below, we only consider the 3WJ analyzed by Thivyanthan et al.,¹⁸ for which an averaged NMR structure is available.¹⁹ It consists of the single strands 3'GCCACGTCG5' (referred to as the X strand), 5'CGGTGCGTCC3' (the H strand), and 5'GGACGTCG-CAGC3' (the R strand), with a total of 32 nucleobases, including twelve guanines. As apparent from the sequences, two consecutive nucleobases of the R strand, C and T, are unpaired. This feature is generally believed to stabilize 3WJs.¹⁵ The structure determined by NMR spectroscopy, as displayed in Figure 2, reflects the influence of the two unpaired bases; it exhibits a T-shape, which is also characteristic of tRNAs, rather than the Y-shape suggested by a naive interpretation of the scheme given in Figure 1. For convenience, we will refer to the gross structural units of the 3WJ as the left, right, and vertical arms, which are joined at a central site or vertex.

A phenomenological hopping model, as developed by Bixon et al.,²⁴ rationalizes DNA hole transport in terms of interbase hopping and trapping as an application of Marcus' theory of charge transfer. From this model, the following picture emerges: fast multistep hopping occurs only between guanine bases, which act as traps due to their low oxidation potential, and intervening A–T base pairs participate in tunneling via a superexchange mechanism. The tunneling probability between two guanines decays exponentially as the number of intervening A–T pairs increases. In addition, Giese and co-workers have introduced elements of long-range transport into their kinetic model due to hopping between adenines.²⁵ This process becomes dominant after two guanines are separated by more than four intervening A–T pairs, and the corresponding charge-transfer rate exhibits a power-law decay with an increasing number of such base pairs. Renger and Marcus have presented an approach that involves tunneling, hopping, and an intermediate regime;²⁶ a related theory for bridge-mediated charge transfer has also been suggested by Petrov et al.²⁷ Recently, Krapf and two of the present authors have demonstrated that the two competing mechanisms suggested for DNA hole transport—superexchange and adenine-adenine hopping—can be derived from the same atomistic model.²⁰ Because this model is used here to estimate the hopping rates between the guanine bases within the 3WJ

described previously, we will briefly review its foundation in the following.

In this work, we assume that the nucleobases with their high-energy frontier molecular orbitals dominate the charge-transport properties, and we hence neglect the deoxyribose and the phosphate units, beyond their role of providing a scaffold for the base pairs. We assume that the σ – π separation approximately holds and that theories of the chemical bond appropriate to π electron systems can be applied. In the field of conductivity phenomena in π systems, the Su–Schrieffer–Heeger (SSH) model²⁸ has a remarkable track of success. In its standard form, the potential energy of the SSH Hamiltonian reads

$$\hat{H} = \sum_{\langle ij \rangle} \frac{k}{2} (x_i - x_j)^2 - \sum_{\langle ij \rangle} [t_0 - \alpha(x_i - x_j)](a_i^\dagger a_j + a_j^\dagger a_i) \quad (2.1)$$

where $x_i - x_j$ denotes the deviation of the distance between a neighboring pair of atoms from that of a C–C single bond, k is the corresponding force constant, t_0 is the tight-binding coupling matrix element, and α denotes the electron–phonon coupling constant. The angular brackets indicate the restriction of the sum to distinct pairs of neighbors, and the a_i^\dagger/a_i are creation/annihilation operators acting on a basis of $2p_z$ atomic orbitals, which is assumed to be orthogonal. As is standard in the SSH model, nuclear coordinates and momenta are treated as classical quantities.

The SSH Hamiltonian can be separated into an electronic component and a nuclear component, using a displaced phonon coordinate.²⁹ Within the restricted Hartree–Fock (HF) mean field approximation, the transformed electronic component of the Hamiltonian is given by²⁹

$$\hat{H} = - \sum_{\langle ij \rangle} (t_0 + 4U_{\text{SSH}}\bar{n}_{ij})(a_i^\dagger a_j + a_j^\dagger a_i) + 4U_{\text{SSH}} \sum_{\langle ij \rangle} \bar{n}_{ij}^2 \quad (2.2)$$

where \bar{n}_{ij} are the tight-binding bond orders (which are proportional to the displacements $x_i - x_j$ of the original SSH Hamiltonian), and we define the so-called off-diagonal Hubbard parameter as $U_{\text{SSH}} = \alpha^2/(2k)$, which is equal to 0.32 meV in the standard SSH model. We define the operator $n_{ij} = a_i^\dagger a_j$, where the terms a^\dagger and a denote the corresponding creation and annihilation operators. The Hamiltonian given in eq 2.2 accounts for the chemical bond within the bases and the inner-sphere contributions to the charge-transfer reaction via a possible change in the bond orders or bond lengths.

To describe the influence of solvent polarization effects, we apply a straightforward extension of Marcus' treatment of the energetics of outer-sphere reactions³⁰ to many-site systems. We write the reorganization energy emerging from an ensemble of excess charges Δz_i localized within spheres of radii σ_i as

$$\lambda_{\text{out}} = \frac{e^2}{4\pi\epsilon_0} \left(\frac{1}{\epsilon_\infty} - \frac{1}{\epsilon_s} \right) \left(\sum_i \frac{\Delta z_i^2}{\sigma_i} - \sum_{i < j} \frac{\Delta z_i \Delta z_j}{r_{ij}} \right) \quad (2.3)$$

If the high- and the low-frequency dielectric response, characterized by the constants ϵ_∞ and ϵ_s , can be separated and the long-range Coulomb interactions are neglected, this model becomes the interaction term of a spin-free Hubbard Hamiltonian.³¹ We replace the charges Δz_i by the corresponding number operators $n_i = n_{ii} = a_i^\dagger a_i$ and arrive at the following mean-field expression:

$$\begin{aligned}\hat{H}_{ee} &= -U_{ee} \sum_i (n_i - n_{i,0})^2 \\ &\simeq -U_{ee} \sum_i [2n_i(\bar{n}_i - \bar{n}_{i,0}) - \bar{n}_i^2 + \bar{n}_{i,0}^2]\end{aligned}\quad (2.4)$$

It can be interpreted as a nonretarded reaction field, which extends the linear combination of atomic orbitals (LCAO) approach to systems embedded in a polarizable environment.^{32,33} In this work, we use $U_{ee} = 0.8$ eV;²⁰ all other parameters have been obtained by a careful fit to ab initio quantum chemical calculations and to the experimental oxidation potentials. Further technical details are given in refs 20 and 21. Because the standard SSH model only describes hydrocarbons, a chemically specific modification has been introduced to handle the heterocyclic nucleobases, which also contain N and O atoms. In addition, interbase tight-binding interactions have been parameterized, and the nucleobases may exhibit an arbitrary mutual orientation. The combined Hamiltonians in eqs 2.2 and 2.4 can be solved self-consistently. In this case, the terms \bar{n}_{ij} and \bar{n}_i are computed from a previous self-consistent field (SCF) step. The limits of this approach are discussed in ref 20; we note, in particular, that we are aware of the facts that (i) DNA may exhibit a distorted geometry at the end of the finite strands studied here, (ii) disorder phenomena may have an important role in charge transfer,^{1,34,35} and (iii) the nonretarded reaction field may find its limits for very fast charge transfer or an extremely slow dielectric or vibrational response.

In the SCF computations, we proceed as follows. Each base is considered to be a potential center of charge localization. Hence, we use initial conditions that reflect the bond order—or bond length—distribution of a single charged base X and that of the neutral bases for the remaining 31 centers; here, X may be varied. Whenever the initial charge is localized on a guanine, the SCF procedure rapidly converges to the final charge distribution. Thus, in the systems studied here, the guanine bases operate as charge traps and form the centers of localization for a polaron state. As a consequence, intermediate A–T pairs act as barriers for tunneling.

We will now quantify these findings by accessing a cross section of the potential energy surface relevant to hole transfer between two guanine bases by a linear synchronous transit (LST) approach.³⁶ In doing so, we adopt a procedure that contains elements of an adiabatic charging process^{37,38} and the application of an interpolation method to charge transfer, which we have recently tested for a multicenter hopping problem.³⁹ The bond orders that characterize each of the minima, which we may denote as X and Y, are given by $\{\bar{n}_{1,1,X}; \bar{n}_{1,2,X}; \dots; \bar{n}_{N-1,N,X}; \bar{n}_{N,N,X}\}$ and $\{\bar{n}_{1,1,Y}; \bar{n}_{1,2,Y}; \dots; \bar{n}_{N-1,N,Y}; \bar{n}_{N,N,Y}\}$, respectively. The interpolation is performed by setting the bond order of the combined Hamiltonians in eqs 2.2 and 2.4 as $\bar{n}_{ij} = \Gamma \bar{n}_{ij,X} + (1 - \Gamma) \bar{n}_{ij,Y}$, where the interpolation parameter Γ serves as a reaction coordinate. The charge orders are interpolated in the same way.

The resulting energy profiles for hole transfer within the 3WJ is displayed in Figure 3. As a reaction coordinate, we use the Γ parameter that we have just referenced and increment its value by one for each consecutive hopping process. On a numerical scale, Γ ranges from 0 to 14 for the sequence of hops considered here. For convenience and for the sake of comparability to Figure 2, we do, however, label the minima of Figure 3—each representing hole localization on a guanine—using the index of the nucleobase in the DNA oligomer.¹⁹ The sequence of hops analyzed here starts at the 5' position of the H strand, i.e., at the left arm, as defined previously. We proceed to the right arm, return, and cross the vertex toward the vertical arm.

The potential energy curves for this scan are displayed in Figure 3. Locally, they exhibit the familiar shape of two parabola

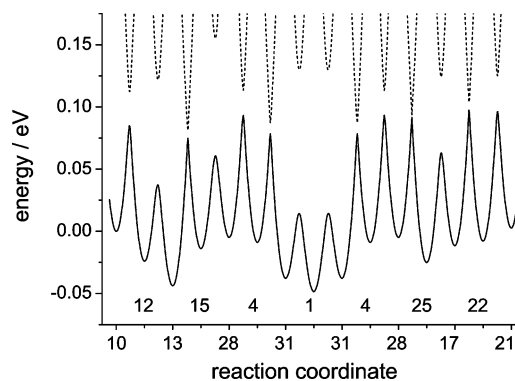


Figure 3. Potential energy surface for hopping processes within the 1EKW 3WJ displayed in Figure 2. Ground state (solid line) and first excited state (dashed line) are shown. Following the reaction coordinate, the labels indicate the guanines on which a positive charge can localize.

that experience a level repulsion. From these curves, effective parameters relevant to Marcus' theory of charge transfer in a two-site donor–acceptor system can be extracted immediately.³³ We obtain the site-specific reorganization energy λ as the difference between the corresponding ground-state minimum and the first excited state. The effective tunnel splitting, $|t|$, is given as half of the difference between the ground state and the excited-state energy at the transition state, i.e., the point of the closest approach between the two curves. In addition, we compute activation barriers E_A for the forward and backward reactions, which include the energy differences between the initial and final states. From these parameters, the hopping rates can be estimated via³⁰

$$k_{CT} = \frac{t^2}{\hbar} \sqrt{\frac{2\pi}{\lambda k_B T}} \exp\left(-\frac{E_A}{k_B T}\right) \quad (2.5)$$

We note that, for high charge-transfer rates, as computed for next-nearest neighbor guanines, nonadiabaticity corrections may apply. In addition, the extremely large hopping rate obtained for nearest-neighbor guanine–guanine transfer suggests complete delocalization over the dimer, as also indicated by experiments that involve cleavage reactions.⁴⁰ However, we are rather interested in particularly slow charge-transfer processes, which constitute the bottlenecks of the overall transfer through the 3WJ. The numerical values computed for all D–A pairs using eq 2.5 are listed in Table 1. Activation barriers range from 60 meV to 120 meV, and the reorganization energies lie in the range of 350–400 meV. In contrast to regular, idealized models of DNA studied using the same Hamiltonian,²⁰ the driving force for charge transfer can amount up to 45 meV. Within a parallel arrangement of nucleobases, the effective tunnel splitting t is dependent on the distance between the guanine donor and acceptor: it can become as large as 47 meV for nearest neighbors. The couplings between the horizontal arms and their vertical counterpart are particularly small: we have 7.7×10^{-3} meV for the most efficient process, 15–25. Here, the participating nucleobases show an orientation that is almost orthogonal and thus slows the CT considerably. For transport along the arms, we observe, as minimum values for t , 2.60 meV within the left arm (13–15), 4.30 meV within the right arm (4–31), and 0.31 meV within the vertical arm (17–22). The charge-transfer rates computed using eq 2.5 are also listed in Table 1. From this calculation, the following orders of magnitude emerge: the rate-limiting step for charge transfer along the horizontal arms is equal to $k_{CT} \approx 10^{11} \text{ s}^{-1}$, whereas hole transfer to the vertical arm is slowed by 4 orders of magnitude, to k_{CT}

TABLE 1: Computed Effective Charge Transfer Parameters for the Three-Way DNA Junction 1EKW^a

D–A pair ^b	Reaction Energy Barrier (meV)		Reorganization Energy (meV)		electronic tunnel splitting, t (meV)	Reaction Coefficient (s ⁻¹)	
	forward, E_A^f	backward, E_A^b	donor, λ_D	acceptor, λ_A		forward, k_{CT}^f	backward, k_{CT}^b
10–12	85.3	109.3	347.0	363.0	1.33×10^1	1.0×10^{13}	3.9×10^{12}
12–13	61.4	81.1	363.0	368.8	4.23×10^1	2.6×10^{14}	1.2×10^{14}
13–15	119.0	89.2	378.8	353.3	2.60×10^0	1.0×10^{11}	3.3×10^{11}
15–28	74.0	65.7	353.3	346.8	4.71×10^1	2.0×10^{14}	2.8×10^{14}
28–4	98.2	102.2	346.8	353.6	1.00×10^1	3.5×10^{12}	3.0×10^{12}
4–31	87.4	116.3	353.6	392.5	4.30×10^0	9.6×10^{11}	3.0×10^{11}
31–1	52.2	62.8	392.5	403.2	5.78×10^1	6.8×10^{14}	4.5×10^{14}
25–17	88.3	74.4	362.3	352.6	3.05×10^1	4.7×10^{13}	8.3×10^{13}
17–22	117.7	103.5	352.6	344.4	3.12×10^{-1}	1.5×10^9	2.7×10^9
22–21	94.1	104.6	344.4	353.0	1.39×10^1	7.9×10^{12}	5.2×10^{12}
15–25	101.3	112.6	353.3	362.3	7.70×10^{-3}	8.0×10^6	1.1×10^6
28–25	97.6	117.8	346.8	362.3	1.52×10^{-3}	3.2×10^4	3.6×10^4
4–25	101.1	117.3	353.6	362.3	7.45×10^{-4}	1.7×10^4	8.9×10^3
15–17	109.1	106.7	353.3	352.6	2.96×10^{-3}	2.0×10^5	2.2×10^5
28–17	105.2	111.8	346.8	352.6	2.60×10^{-4}	1.8×10^3	1.4×10^3
4–17	108.8	111.4	353.6	352.6	1.04×10^{-3}	2.4×10^4	2.2×10^4

^a Data taken from refs 18 and 19. All values obtained at a temperature of $T = 298$ K. ^b Donor and acceptor guanine indices (see Figure 2).

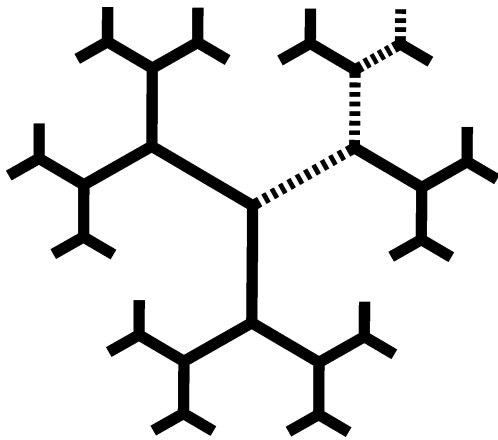


Figure 4. Schematic diagram of a dendrimer at generation $g = 3$ as a regular structure incorporating 3WJs. The fast conductivity path discussed in the text is drawn as a dashed line.

$\approx 10^7$ s⁻¹. In the following section, we will use these rates to discuss charge transfer in nanosized objects that feature 3WJs as their main building blocks. Because the 3WJ studied by van Buuren et al.²² contains guanines in positions less favorable to promote an efficient CT, we focus here only on the geometry presented by Thivyanathan and co-workers.¹⁸

3. DNA Networks

In this section, we will address the problem of charge transport within DNA dendrimers. From a topological perspective, these objects are trees, because they lack loops. This feature is particularly important when considering their behavior in solution, as was discussed in ref 41 for finite Sierpinski fractals and in ref 42 for regular hyperbranched polymers.⁴³ Being topologically equivalent to finite Cayley trees, the dendrimers are constructed from a core with f branches (f denotes the coordination number), to which $f - 1$ new branches are attached in the next stage of a recursive construction. As an example, we present in Figure 4 a dendrimer with $f = 3$ —as relevant to DNA—for the third iteration step of generation g . Because of the exponential increase in the number of branches at each generation, the chemical synthesis usually terminates after five or six recursive steps. Many dynamical properties of polymers—such as the vibrational spectrum, the relaxation modes, the linear

dielectric properties and random walk aspects (on which we focus here)—are dependent on the eigenvalues of the corresponding connectivity matrices. For dendrimers of arbitrary size, these eigenvalues can be obtained semianalytically using powerful factorization methods for the characteristic polynomials and thus avoiding the need to diagonalize the connectivity matrices numerically.^{44–46}

In DNA charge transfer, guanine clusters G_n ($n \geq 2$) act as traps for migrating holes and as centers for consecutive DNA cleavage reactions.^{1,3} In the following, we will consider dendrimers of varying size g with a charge donor located on one of the peripheral sites and a central absorbing trap with a high content of G_n clusters. As a simplification, side reactions that involve intervening guanines are ignored. However, they can be fully taken into account by a numerical solution of the rate equations, as defined below. Within the network, we represent each 3WJ by its center (the vertex) and three bonds. Hopping between the vertexes is described by the corresponding rate-limiting processes, with rates as computed using an atomistic model of the 3WJs in the previous section; here, we use $k_f = 10^{11}$ s⁻¹ and $k_s = 10^7$ s⁻¹. As compared to the previous section, hopping processes are thus described on a more coarse-grained length scale: the interbase hopping processes are now replaced by intervertex transport, and this strategy enables an effective numerical solution of the transport problem, as described in the following.

For a description of the overall charge-transfer process, we introduce the vertexes V_1, V_2, \dots, V_n along one arm of the dendrimer. V_1 denotes a peripheral 3WJ labeled by a donor and V_n denotes a central trap. Two vertexes can be connected by a bond enabling fast CT or by a bond that is characterized by a slow CT, and each vertex forms the center of bonds for two slow processes and a single fast one. By a careful design of the individual protruding 3' and 5' 3WJ ends (cf. Figure 1), it is possible to construct an object that exhibits a fast conducting path between the donor and the trap which is decorated only by bonds that exhibit a slow CT. In this case, because of the high ratio $k_f/k_s = 10^4$, the transport problem resembles that of a linear chain with $n = g + 1$ sites, and we have

$$V_1 \rightleftharpoons V_2 \rightleftharpoons \dots \rightleftharpoons V_{n-2} \rightleftharpoons V_{n-1} \rightarrow V_n \quad (3.1)$$

where the last process is irreversible. The corresponding hopping kinetics can be described by a system of coupled linear

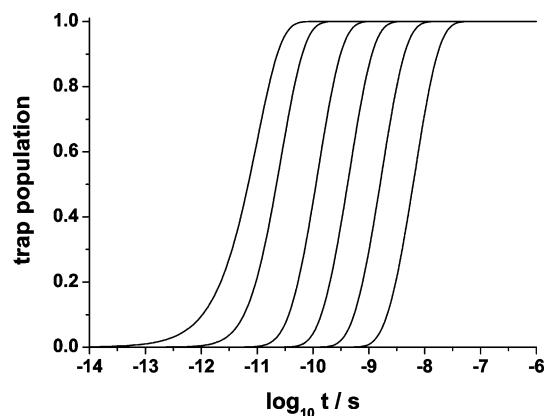


Figure 5. Probability of finding a positive charge at the central trap of a donor–acceptor system. From left to right: dendrimers at generation $g = 1, 2, 5, 10, 20$, and 40 .

homogeneous first-order rate equations. The individual equations that specify the changes of the hole populations $P_i(t)$ on sites V_i read

$$\dot{P}_1(t) = -k_{1,2}P_1(t) + k_{2,1}P_2(t) \quad (\text{for the donor site, } i = 1) \quad (3.2)$$

$$\dot{P}_i(t) = k_{i-1,i}P_{i-1}(t) - (k_{i,i+1} + k_{i,i-1})P_i(t) + k_{i+1,i}P_{i+1}(t) \quad (\text{for } 1 < i < n - 1) \quad (3.3)$$

$$\dot{P}_{n-1}(t) = k_{n-2,n-1}P_{n-2}(t) - (k_{n-1,n} + k_{n-1,n-2})P_{n-1}(t) \quad (\text{for the site adjacent to the central trap, } i = n - 1) \quad (3.4)$$

and

$$\dot{P}_n(t) = k_{n-1,n}P_{n-1}(t) \quad (3.5)$$

for the central trap. For all reaction coefficients, we have $k_{i,i\pm 1} = k_f$. We make the familiar ansatz $P_i(t) = p_i \exp(-\lambda t)$, where p_i is independent of t , and arrive at the eigenvalue problem:

$$(-\mathbf{K} - \lambda \mathbf{1})\vec{p} = \vec{0} \quad (3.6)$$

which leads to the eigenvalues λ_α and the eigenvectors \vec{p}_α . Here, \mathbf{K} denotes the tridiagonal matrix of reaction coefficients, $k_{i,i\pm 1}$. The populations, as a function of time, are given by

$$\vec{P}(t) = \sum_{\alpha} c_{\alpha} \vec{p}_{\alpha} \exp(-\lambda_{\alpha} t) \quad (3.7)$$

where the coefficients c_{α} are computed to fulfill the initial condition $P_i(t = 0) = \delta_{i,1}$, corresponding to complete charge localization on the donor. We note that $\lambda_{\alpha} > 0 \forall \alpha$. For isotropic transport through the junctions, the trapping problem permits an effective semianalytical solution, as demonstrated by Bar-Haim et al. with the application to energy transfer in light-harvesting antenna complexes.⁴⁷

In Figure 5, we present the population of the central trap as a function of time for dendrimers of various size, as characterized by the number of generations g used for their construction ($g = 1, 2, 5, 10$, and 20). To each g value, a characteristic time scale $t_{1/2}$ can be attributed, at which, on average, half of the excess charge is located within the trap. This time increases as the system size increases: the half-lives range from $-\log t_{1/2} = 10.6$ s for $g = 1$ to $-\log t_{1/2} = 8.8$ s for $g = 20$. Thus, even very large objects enable transport to the central trap that is

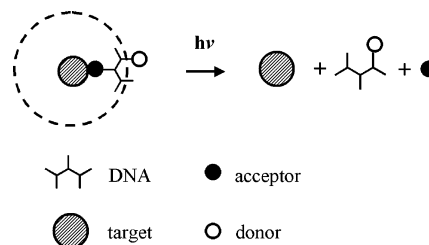


Figure 6. Outline of a DNA-based drug-delivery system. (For details, see text.)

fast, compared to the consecutive oxidation and fragmentation of the DNA with $k_{ox} \leq 10^{-8} \text{ s}^{-1}$,³ which is consequently almost size-independent up to $g = 20$. For dendrimers, this size has to be interpreted as a purely formal quantity, as the spatial requirements limit the size to $g = 5$ or 6 . We note that scaling, self-similar objects with the same connectivity, such as regular hyperbranched polymers, can overcome this limitation.^{42,43,48}

As a material, DNA shows a high biocompatibility and may thus be used in pharmaceutical applications. In the following, we derive a sketch of a DNA-based drug delivery system that utilizes the aforementioned properties of a rapid peripheral donor–central trap CT system. Its basic elements are displayed in Figure 6: a DNA-binding target, such as a DNA intercalate or a DNA or RNA fragment, is connected to a protective DNA or RNA coating with a specifically designed shape or size via at least one DNA or RNA fragment, which operates as a charge trap (e.g., polyguanine sequences or artificial bases such as methylindole). Upon irradiation, oxidative stress, or other initialization processes, a positive charge is transferred from the peripheral donor to the charge trap, where consecutive oxidation and DNA cleavage occurs, the target molecule is now released and becomes active. This system may find an application for all cell types into which nanosized DNA objects can be easily incorporated and that can be effectively irradiated. As an example, one may think about a transfer of DNA-bound cytostatics or DNA fragments using this carrier into suspended cells, within cell cultures or into the epidermis (e.g., via iontophoresis), followed by a controlled release via laser irradiation.

4. Conclusions

Motivated by recent progress in the design of complex, branched DNA oligomers, the corresponding structural analysis, and first experiments of charge transfer along DNA junctions,^{16,17} we have approached transport processes within DNA dendrimers from a theoretical and numerical perspective. To predict hopping rates for large systems quantitatively, we have used a two-level hierarchy of models.

To describe the electronic structure of an isolated three-way junction (3WJ) based on a NMR structure, we have applied an extended Su–Schrieffer–Heeger model. This model is atomistic and, hence, chemically specific; considers both inner-sphere and outer-sphere reorganization degrees of freedom, and has been carefully parametrized using ab initio quantum chemical computations and experimental data. In a mean-field approach to this model, we have computed the potential energy surfaces that are dependent on the expectation values of the charge and the bond orders. Because of their low oxidation potential, guanines form the centers of attraction for an excess positive charge within a self-consistent field calculation. The corresponding polaron states serve as minima for a linear synchronous transit approach to the potential energy surface, from which the relevant

Marcus parameters (activation barriers, reorganization energy, and effective tunnel splitting) have been extracted. From these quantities, interguanine superexchange hopping rates have been computed, which ultimately reflect the T-shaped anisotropy of the 3WJ via two different rate-limiting reaction coefficients along the branches of the oligomer, $k_f \approx 10^{11} \text{ s}^{-1}$ and $k_s \approx 10^7 \text{ s}^{-1}$.

These rates serve as input parameters to a classical kinetic description of charge transport within a dendrimer network of 3WJs, which constitutes the second level of our model. We apply a coarse-grained description that interprets 3WJs as vertexes that are connected by bonds with anisotropic hopping rates, which are given by the rate-limiting reaction coefficients. A particular realization of this model has been studied in detail: a peripheral charge donor is connected to a central absorbing trap by a chain of bonds, enabling fast charge transfer. In turn, this model can be treated with high accuracy as a linear chain, which is separated from the other branches of the dendrimer by contacts that only permit slow transfer or that are disconnected from this branch by the central trap. Up to a hypothetical generation of $g = 20$, charge transfer along the selected branch is faster than the oxidation and fragmentation processes occurring at the central site. As a potential application for biocompatible drug delivery based on a branched charge-transfer system, we have considered a target connected to a protective coating by G-rich DNA fragments that is released upon oxidation initiated by a remote peripheral donor.

Whereas previous applications of our model have essentially reproduced experimental findings for charge transfer along DNA oligomers²⁰ and through the nucleosome,²¹ we now make quantitative predictions that can be tested on each level of the model. First, charge transfer through the isolated junction studied here should be highly anisotropic, with rates differing by a factor of 10^4 . Second, even for large dendrimers of these 3WJs that contain the design element of a fast conducting path, a central G-rich trap can be reached prior to the oxidation of intervening G_n clusters. This leads to a strong contribution to the fragmentation of the dendrimer by three roughly equi-sized parts that can be identified by gel electrophoresis. An experiment that closely resembles the first approach toward verification, but involves a different, more isotropic 3WJ has recently been described by Santhosh and Schuster.¹⁶ In addition to direct donor–acceptor charge transfer, a small amount of charge migration along the junction has been observed, but not quantified. To enhance the efficiency of this process, we suggest a specific design that embodies a stabilized T-shaped junction with guanines located close to the center of the structure.

Acknowledgment. It is a pleasure to thank L. Engel, Chr. von Ferber, Th. Friedrich, G. Ganzenmüller, A. Jurjiu, S. Larsson, E. Neumann, M. Rateitzak, C. A. M. Seidel, E. B. Starikov, N. Utz, and C. A. Zell for fruitful discussions and helpful comments. We gratefully acknowledge financial support by the Deutsche Forschungsgemeinschaft via the SFB Strukturierte Makromolekulare Netzwerksysteme. A.B. acknowledges the support of the Fonds der Chemischen Industrie.

References and Notes

- (1) (a) Treadway, C. R.; Hill, M. G.; Barton, J. K. *Chem. Phys.* **2002**, *281*, 409. (b) Delaney, S.; Barton, J. K. *J. Org. Chem.* **2003**, *68*, 6475.
- (2) Fink, H.-W. *Cell. Mol. Life Sci.* **2001**, *58*, 1.
- (3) Schuster, G. B. Long-Range Charge Transfer in DNA. *Top. Curr. Chem.* **2004**, *236*.
- (4) Endres, R. G.; Cox, D. L.; Singh, R. R. P. *Rev. Mod. Phys.* **2004**, *76*, 195.
- (5) (a) Arkin, M. R.; Stemp, E. D. A.; Holmlin, R. E.; Barton, J. K.; Hoermann, A.; Olson, E. J. C.; Barbara, P. F. *Science* **1996**, *273*, 475. (b) Hall, D. B.; Holmlin, R. E.; Barton, J. K. *Nature* **1996**, *382*, 731.
- (6) (a) Fiebig, T.; Wan, C.; Kelley, S. O.; Barton, J. K.; Zewail, A. H. *Proc. Natl. Acad. Sci.* **1999**, *96*, 1187, 6014. (b) Wan, C.; Fiebig, T.; Schiemann, O.; Barton, J. K.; Zewail, A. H. *Proc. Natl. Acad. Sci.* **2000**, *97*, 14052.
- (7) (a) Meggers, E.; Kusch, D.; Spichty, M.; Wille, U.; Giese, B. *Angew. Chem., Int. Ed.* **1998**, *37*, 459. (b) Meggers, E.; Michel-Beyerle, M. E.; Giese, B. *J. Am. Chem. Soc.* **1998**, *120*, 12950.
- (8) (a) Fink, H. W.; Schönenberger, C. *Nature* **1999**, *398*, 407. (b) Porath, D.; Bezryadin, A.; de Vries, S.; Dekker, C. *Nature* **2000**, *403*, 635.
- (9) See, e.g., de Pablo, P. J.; Moreno-Herrero, F.; Colchero, J.; Herrero, J. G.; Herrero, P.; Baró, A. M.; Ordejón, P.; Soler, J. M.; Artacho, E. *Phys. Rev. Lett.* **2000**, *85*, 4992.
- (10) Chen, J.; Seeman, N. C. *Nature* **1991**, *350*, 631.
- (11) Shih, W. M.; Quispe, J. D.; Joyce, G. F. *Nature* **2004**, *427*, 618.
- (12) Wang, J.; Jiang, M.; Nilsen, T. W. *J. Am. Chem. Soc.* **2000**, *122*, 1848.
- (13) Li, Y.; Tseng, Y. D.; Kwon, A. Y.; D'Espaux, L.; Bunch, J. S.; McEuen, P. L.; Luo, D. *Nature Mater.* **2004**, *3*, 38.
- (14) Luo, D. *Mater. Today* **2003**, *6* (11), 38–43.
- (15) Gao, X.; Stassinopoulos, A.; Ji, J.; Kwon, Y.; Bare, S.; Goldberg, I. H. *Biochemistry* **2002**, *41*, 5131.
- (16) Santhosh, U.; Schuster, G. B. *Nucleic Acid Res.* **2003**, *31*, 5692.
- (17) (a) Odom, D. T.; Dill, E. A.; Barton, J. K. *Nucleic Acid Res.* **2001**, *29*, 2026. (b) Nunez, M. E.; Noyes, K. T.; Gianolio, D. A.; McLaughlin, L. W.; Barton, J. K. *Biochemistry* **2000**, *39*, 6190.
- (18) Thiviyanathan, V.; Luxon, B. A.; Leontis, N. B.; Illangasekare, N.; Donne, D. G.; Gorenstein, D. G. *J. Biomol. NMR* **1999**, *14*, 209.
- (19) Protein Database (PDB) Entry 1EKW.
- (20) Cramer, T.; Krapf, S.; Koslowski, Th. *J. Phys. Chem. B* **2004**, *108*, 11812.
- (21) Cramer, T.; Krapf, S.; Koslowski, Th. *Phys. Chem. Chem. Phys.* **2004**, *6*, 3260.
- (22) van Buuren, B. N. M.; Overmars, F. J. J.; Ippel, J. H.; Altona, C.; Wijmenga, S. S. *J. Mol. Biol.* **2000**, *304*, 371.
- (23) Protein Database (PDB) Entry 1EZK.
- (24) Bixon, M.; Giese, B.; Wessely, S.; Langenbacher, T.; Michel-Beyerle, M. E.; Jortner, J. *Proc. Natl. Acad. Sci.* **1999**, *96*, 11713.
- (25) (a) Giese, B.; Amaudrut, J.; Kohler, A. K.; Spormann, M.; Wessely, S. *Nature* **2001**, *412*, 318. (b) Giese, B.; Spichty, M. *ChemPhysChem* **2000**, *1*, 195.
- (26) Renger, T.; Marcus, R. A. *J. Phys. Chem. A* **2003**, *107*, 8404.
- (27) Petrov, E. G.; Shevchenko, Ye, V.; May, V. *Chem. Phys.* **2003**, *288*, 269.
- (28) Su, W. P.; Schrieffer, J. R.; Heeger, A. J. *Phys. Rev. Lett.* **1979**, *42*, 1698; *Phys. Rev. B* **1980**, *22*, 2099.
- (29) Rateitzak, M.; Koslowski, Th. *Chem. Phys. Lett.* **2003**, *377*, 455.
- (30) Marcus, R. A. *J. Chem. Phys.* **1956**, *24*, 966, 979; *Annu. Rev. Phys. Chem.* **1964**, *15*, 155.
- (31) (a) Micnas, R.; Ranninger, J.; Robaskiewicz, S. *Rev. Mod. Phys.* **1990**, *62*, 113; Shen, S.-Q. *Int. J. Mod. Phys. B* **1998**, *12*, 709. (b) Mancini, F.; Marinaro, M.; Matsumoto, H. *Int. J. Mod. Phys. B* **1996**, *10*, 1717. (c) Georges, A.; Kotliar, G.; Krauth, W.; Rozenberg, M. J. *Rev. Mod. Phys.* **1996**, *68*, 13.
- (32) Utz, N.; Koslowski, Th. *Chem. Phys.* **2002**, *282*, 389.
- (33) Koslowski, Th. *J. Chem. Phys.* **2000**, *113*, 10703; *Z. Phys. Chem. (Muenchen)* **2001**, *215*, 1625; *Phys. Chem. Chem. Phys.* **2003**, *5*, 2197.
- (34) Voityuk, A. A.; Siri Wong, K.; Rösch, N. *Phys. Chem. Chem. Phys.* **2001**, *3*, 5421.
- (35) Voityuk, A. A.; Siri Wong, K.; Rösch, N. *Angew. Chem., Int. Ed.* **2004**, *43*, 624.
- (36) (a) Rauhut, G.; Clark, T. *J. Am. Chem. Soc.* **1993**, *115*, 9127. (b) Gröppel, M.; Roth, W.; Clark, T. *Adv. Mater.* **1995**, *7*, 927.
- (37) Hwang, J.-K.; Warshel, A. *J. Am. Chem. Soc.* **1987**, *109*, 715.
- (38) (a) Kuharski, R. A.; Bader, J. S.; Chandler, D.; Sprik, M.; Klein, M. L.; Impey, R. W. *J. Chem. Phys.* **1988**, *89*, 3248. (b) Bader, J. S.; Chandler, D. *Chem. Phys. Lett.* **1989**, *157*, 501. (c) Bader, J. S.; Kuharski, R. A.; Chandler, D. *J. Chem. Phys.* **1990**, *93*, 230.
- (39) Koslowski, Th.; Jurjiu, A.; Blumen, A. *J. Phys. Chem. B* **2004**, *108*, 3283.
- (40) O'Neill, P.; Parker, A. W.; Plumb, A. A.; Siebbeles, L. D. A. *J. Phys. Chem. B* **2001**, *105*, 5283.
- (41) Jurjiu, A.; Koslowski, Th.; Blumen, A. *J. Chem. Phys.* **2003**, *118*, 2398.
- (42) Jurjiu, A.; Koslowski, Th.; von Ferber, Chr.; Blumen, A. *Chem. Phys.* **2003**, *294*, 187.
- (43) Blumen, A.; von Ferber, Chr.; Jurjiu, A.; Koslowski, Th. *Macromolecules* **2004**, *37*, 638.

- (44) Cai, C.; Chen, Z. Y. *Macromolecules* **1997**, *30*, 5104.
- (45) Gurtovenko, A. A.; Gotlib, Yu. Ya.; Blumen, A. *Macromolecules* **2002**, *35*, 7481.
- (46) Gurtovenko, A. A.; Markelov, D. A.; Gotlib, Yu. Ya.; Blumen, A. *J. Chem. Phys.* **2003**, *119*, 7579.
- (47) (a) Bar-Haim, A.; Klafter, J.; Kopelman, R. *J. Am. Chem. Soc.* **1997**, *119*, 6197. (b) Bar-Haim, A.; Klafter, J. *J. Phys. Chem. B* **1998**, *102*, 1662.
- (48) Blumen, A.; Jurjiu, A.; Koslowski, Th.; von Ferber, Chr. *Phys. Rev. E* **2003**, *67*, 061103.